Heliyon 10 (2024) e23562

Contents lists available at ScienceDirect

Heliyon

journal homepage: www.cell.com/heliyon

Investigation of intermolecular interactions of L-Valine and L-Phenylalanine with muscle relaxant drug mephenesin molecule prevalent in aqueous solution by various physico-chemical methods at T=298.15K–313.15K

Baishali Saha [a], Sanjoy Barman [a], Sukdev Majumder [a], Biswajit Ghosh [a], Kangkan Mallick [a], Subhankar Choudhury [b], Mahendra Nath Roy [a,c,*]

[a] Department of Chemistry, University of North Bengal, Darjeeling, 734013, India
[b] Department of Chemistry, Malda College, Malda, 732101, India
[c] Vice-Chancellor, Alipurduar University, Alipurduar 736121, 734013, Darjeeling, India

ARTICLE INFO

Keywords:
Mephenesin
L-Valine
L-Phenylalanine
Solute-solvent interaction
Proton NMR study
Computational study

ABSTRACT

A complete chemical analysis of significant intermolecular interactions of L-Valine (L-Val) and L-Phenylalanine (L-Phe) with Mephenesin (MEPN) molecules in aqueous solution has been studied by different physicochemical methodologies at various temperatures (T = 298.15 K–313.15 K at an interval of 5 K) and concentrations (0.001 mol kg^{-1}, 0.003 mol kg^{-1}, 0.005 mol kg^{-1}) of aqueous MEPN solution. The limiting apparent molar volume ($\varphi_V{}^0$) and experimental slope ($S_V{}^*$) values are found from the equation of Masson, viscosity A and B-coefficient determined using the equation of Jones-Doles, molar refraction (R_M) and limiting molar refraction (R_M^0) derived by the Lorentz-Lorenz equation, express that in our experimental solution of amino acids (AAs) in aqueous MEPN, the solute-solvent interaction predominates over the solute-solute and solvent-solvent interactions for these ternary solutions. These are also justified by the measurement of various thermodynamic parameters, free energy of activation of viscous flow per mole of solvent ($\Delta\mu_1{}^\circ\#$) and solute ($\Delta\mu_2{}^\circ\#$), activation of viscous flow of enthalpies ($\Delta H^\circ\#$) and entropies ($\Delta S^\circ\#$). The characteristics of structure-breaking of solutes in the aqueous drug solution have been identified by Hepler's method and dB/dT value. The spectroscopic methods like UV–visible and proton-NMR studies help to explicate the strong AA-MEPN interactions in the solution phase and obtain a good correlation with theoretical studies. Theoretical investigations are checked to authenticate the experimental observations and according to both studies, L-Phe-MEPN interaction is greater than L-Val-MEPN interaction. The experimental and correlated research data are useful for the development of model combinations of AAs with drug molecules in pharmaceutical and medicinal chemistry.

1. Introduction

The Macromolecule-Drug interaction in a water medium takes part in a vital role in the biochemical process and provides

* Corresponding author. Department of Chemistry, University of North Bengal, Darjeeling, 734013, India.
E-mail addresses: mahendraroy2002@yahoo.co.in, vcapduniversity@gmail.com (M.N. Roy).

https://doi.org/10.1016/j.heliyon.2023.e23562
Received 19 September 2023; Received in revised form 6 December 2023; Accepted 6 December 2023
Available online 12 December 2023

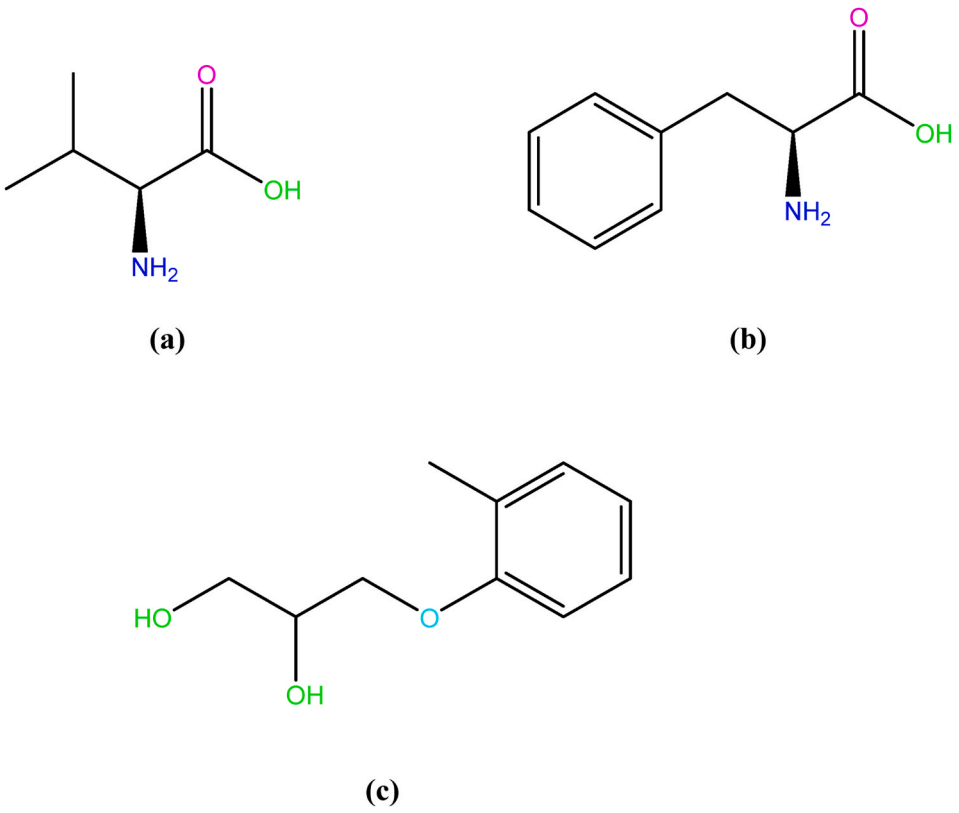

Scheme 1. Molecular structures of L-Valine (a), L-Phenylalanine (b) and Mephenesin (c).

noteworthy ideas like the attaching of drugs with the structure of proteins, transportation of a drug, and therapeutic action of a drug to the desired target [1]. This type of interaction affects the influence of the drug in the body of a living organism due to the receptor nature of drug molecules toward proteins as it has a difficult three-dimensional structure exhibiting different chemical properties [2]. The recent perception of biological macromolecules topic is unacceptable without being vigilant of the solvent atmosphere because hydration by water molecules explains a key function in the gathering of the three-dimensional construction of dynamic protein. The significant output in forming the stable native structures of biopolymers depends on the hydration of the hydrophobic part, charged functional groups, and an ionic portion which are the components of every biological system [3]. The biochemical processes consist of volume change and hydration of biological macromolecules in water, so the various thermodynamic studies and transportation of biomolecules like amino acids, vitamins, and sugars in aqueous drug solutions distribute fruitful data in medicinal and pharmaceutical chemistry [4]. The interactions of non-covalent types like ion-ion, hydrophobic-hydrophobic, dipole-dipole, ion-dipole, and hydrogen bonding arise in solution, play an important part in the formation of the stable complex structure of proteins and lead a role in increasing the stability [5]. In recent research work, the experimentation and computational investigations of the alpha-AAs, viz., L-Valine (L-Val), L-Phenylalanine (L-Phe) (Scheme 1) in aqueous solution of Mephenesin have been done to detect probable interactions predominant in these type of ternary mixtures which can sustain the life metabolism with technical applications of drugs in aqueous phase by providing beneficial data [6–11].

The drug belongs to the glycerol ether family, significantly most useful is Mephenesin (MEPN) (Scheme 1), a chemically known as 3-(2-methylphenoxy)propane-1,2-diol which is used as a centrally operating relaxant used for skeletal muscle anticonvulsant, local anesthesia, and muscle paralyzer [12]. The colourless, odourless, crystalline solids of MEPN have a specific action on spinal interneurons with contractions of polysynaptic reflexes and unaltered reflexes of monosynaptic knee-jerk [13].

Amino acids (AAs), the construction units of protein have a central role in biochemistry, and many functions in metabolism and nutrition [14]. L-Val is in the category of essential AA, i.e., a person can require its need from foods by consuming and gaining from dietary resources that help in the growth and regeneration of muscle, produce energy, increase endurance, and recover muscle tissue. L-Phe also belongs to the essential AA family and is a component of vital protein structures and enzymes, it transforms into Tyrosine by the body, which can be used to synthesize Dopamine and Norepinephrine neurotransmitters. These AAs appear as zwitter ions in a water medium at neutral pH and have a large dipole moment that can interact with solvents having a dipolar nature and authorizes the stability and denaturation process of proteins because of the size, hydrophobicity, and reactivity of AAs [15].

In our current work, we have reported the methodical determinations of density, ρ, viscosity, η, refractive index, n_D, conductance, Λ, and surface tension, σ of L-Val and L-Phe in an aqueous solution of MEPN at altered concentrations (molality), temperatures and at atmospheric fixed pressure targeting to explain solute-solvent interactions prevailing in the investigated medium and to obtain the

effect of variation on the phenomena of physicochemical manners of the aqueous drug solution in presence of both the AAs. With the help of these observations, we have calculated limiting molar apparent volume ($\varphi_V{}^0$), Jones-Dole coefficients (B), Falkenhagen coefficient(A), Hepler's constant (dB/dT), free energy of activation of viscous flow per mole of solvent ($\Delta\mu_1{}^\circ\#$) and solute ($\Delta\mu_2{}^\circ\#$), enthalpies ($\Delta H^\circ\#$) and entropies ($\Delta S^\circ\#$) of activation of viscous flow to explain the solute-solvent interaction among them in a better way and the experimental values are well supported by spectroscopic methods of UV–Vis and proton NMR study. L-Phe-MEPN interactions are observed to be greater than L-Val-MEPN interactions by experimental as well as theoretical data.

DFT study is applied to find out the geometries of optimization, maps of molecular electrostatic potential (ESP), and reduced density gradient (RDG) determination. Our theoretical data and experimental observations correlate with each other.

2. Experimental segment

The chemicals were collected from various recognized chemical sources to perform this research work. The chemicals were always reserved in the desiccators over P_2O_5 in dry condition. The features of the purchased chemicals which we used in this research work, were written in Table S1. Selected chemicals were utilized as purchased, no further purification was done and these solutions were made up with doubly distilled water.

2.1. Equipment and methods

Formerly to begin the investigational work, solubility has been tested out precisely for our selected drug Mephenesin and two AAs L-Val and L-Phe in deionized and triply distilled water. The preparation of an aqueous MEPN solution which was used as a solvent was done by mass with the assistance of Mettler Toledo AG-285 having uncertainty ±0.01 mg. Stock solutions of used AAs were arranged by mass in aqueous MEPN solution and then the required solutions of six different sets were also obtained by mass dilution from the prepared mother solution. For continuing the proper work, always new solutions were prepared. At first, we prepared the drug solutions of 0.001 mol kg^{-1}, 0.003 mol kg^{-1}, and 0.005 mol kg^{-1} in 500 mL water. Then 0.1 mol kg^{-1} L-Val and 0.1 mol kg^{-1} L-Phe were organized in the aqueous MEPN solutions. We set up and utilized: 30 mL each, 0.001 mol kg^{-1} MEPN +0.1 mol kg^{-1} AA in six test tube sets (0.010, 0.025, 0.040, 0.055, 0.070, 0.085 mol kg^{-1} by dilution), 0.003 mol kg^{-1} MEPN + 0.1 mol kg^{-1} amino acid in six sets (0.010, 0.025, 0.040, 0.055, 0.070, 0.085 mol kg^{-1} by dilution), 0.005 mol kg^{-1} MEPN + 0.1 mol kg^{-1} amino acid in six sets (0.010, 0.025, 0.040, 0.055, 0.070, 0.085 mol kg^{-1} by dilution) at $T = 298.15$ K–313.15 K temperature for experimental intention. Overall standard uncertainty in molality according to the mass purity of the studied samples is to be ±0.0083 mol kg^{-1}.

The molarity of the AA in aqueous MEPN solution has been exchanged into molality by using the mathematical equation-1 [16].

$$m = \frac{1}{\left\{\left(\frac{\rho}{c}\right) - \left(\frac{M}{1000}\right)\right\}} \tag{1}$$

where m denotes the molality, ρ represents density, and the molarity (mol/L) of the investigated solution is represented by c and M depicts the relative molar mass of the solute samples.

A vibrating U-tube Anton Paar digital density meter (DMA 4500 M), which has a precision value of ±0.01 kg m^{-3}, was used to evaluate the densities of the solutions (ρ) sustained at ±0.01 K in the temperature region of $T = 298.15$ K–313.15 K with an interval of 5 K. The calibration of the density meter was done with triple-time distilled water and by fanning with dry air earlier than checking the readings of every individual experimental set. The densities of pure water used in calibration at 298.15 K, 303.15 K, 308.15 K, 313.15 K were 997.05 kg m^{-3}, 995.65 kg m^{-3}, 994.04 kg m^{-3}, 992.24 kg m^{-3} respectively. The overall uncertainity in density measurement was calcutated to be about ±0.150 kg m^{-3}.

The viscosity values (η) for all the prepared sets were analyzed with the Ultra Programmable Rheometer machine of Brookfield DV-III, which has a spindle size of 42, solving the numerical equation written where η is related to spindle torque (torque):

$$\eta = (100 / \mathrm{RPM}) \times \mathrm{TK} \times \mathrm{torque} \times \mathrm{SMC} \tag{2}$$

in this following equation-2, RPM represents the speed, TK (0.09373) depicts the constant term of viscometer torque and SMC (0.327) denotes the constant of the spindle multiplier respectively and these values were provided in the viscometer software. The calibration checked for the device by utilizing recognized samples, H_2O, and ($CaCl_2$+ H_2O) as selecting references. Previous to performing any experimentation, we checked calibration to stay away from pointless errors. The temperature for each solution was controlled and monitored for every experimental observation by a thermostat bath of Brookfield Digital TC-500. Viscosity (η) values were evaluated with ±0.1 % accuracy. The overall uncertainty in viscosity was to be about ±0.035 mPa s.

The LED-attaching digital refractometer Mettler Toledo which has $\lambda = 589.3$ nm source light was utilized to take the refractive index values. The instrument was calibrated twice with distilled H_2O when we took the observations for an individual solution. The overall uncertainity was ±0.0032 units for refractive index determination.

The conductivity value of the experimental solutions was determined by Systronics-308 Conductivity Bridge and an immersion conductivity cell of CD-10 dip-type with a cell constant value of nearly 0.100 ± 0.001 cm^{-1}. We calibrated the conductivity cell by utilizing the Lind et al. method [17]. The determined specific conductivity of deionized and triply distilled water at 298.15 K, 303.15 K, 308.15 K, 313.15 K were 2.090 μS cm^{-1}, 2.470 μS cm^{-1}, 2.850 μS cm^{-1}, 3.230 μS cm^{-1} respectively. Before starting the experiment, the conductivity cell was also calibrated at a particular temperature with the use of a newly made-up 0.001 M (KCl + H_2O) mixture.

Table 1
Limiting apparent molar volume ($\varphi_V{}^0$), Regression Co − efficient (R2), Experimental slope ($S_V{}^*$), Viscosity-*B* and Viscosity-*A* coefficient term, and Limiting molar Refraction (R_M^0) of (L-Val + aqueous MEPN) and (L-Phe + aqueous MEPN) systems of altered concentrations (molality) of MEPN in aqueous solution at changing temperatures.

Temperature T (K[b])	$\varphi_V{}^0 \times 10^6$ (m^3 mol^{-1})	R^2	$S_V{}^* \times 10^6$ (m^3 $mol^{-3/2}$ $kg^{1/2}$)	B (dm^3 mol^{-1})	A ($dm^{3/2}$ $mol^{-1/2}$)	R_M^0 (m^3 mol^{-1})
0.001 *m*[a]	**(L- Val + aqueous MEPN) system**					
298.15	93.336 ± 0.000	0.997	−9.469 ± 0.000	0.4387 ± 0.0037	0.1343 ± 0.0018	24.080 ± 0.002
303.15	95.053 ± 0.000	0.999	−14.818 ± 0.001	0.5077 ± 0.0041	0.1320 ± 0.0023	24.101 ± 0.002
308.15	96.690 ± 0.001	0.998	−19.465 ± 0.002	0.6192 ± 0.0051	0.1282 ± 0.0032	24.133 ± 0.003
313.15	98.055 ± 0.001	0.996	−22.934 ± 0.001	0.7465 ± 0.0063	0.1260 ± 0.0033	24.157 ± 0.003
0.003 *m*[a]	**(L- Val + aqueous MEPN) system**					
298.15	94.689 ± 0.001	0.997	−12.889 ± 0.002	0.5322 ± 0.0044	0.1312 ± 0.0030	24.090 ± 0.003
303.15	96.567 ± 0.000	0.998	−19.769 ± 0.001	0.5989 ± 0.0054	0.1287 ± 0.0028	24.112 ± 0.002
308.15	97.871 ± 0.001	0.999	−21.597 ± 0.002	0.7224 ± 0.0057	0.1266 ± 0.0049	24.144 ± 0.003
313.15	99.310 ± 0.001	0.999	−24.332 ± 0.002	0.8626 ± 0.0073	0.1241 ± 0.0037	24.167 ± 0.003
0.005 *m*[a]	**(L- Val + aqueous MEPN) system**					
298.15	95.984 ± 0.001	0.998	−16.226 ± 0.000	0.6358 ± 0.0041	0.1279 ± 0.0034	24.095 ± 0.002
303.15	98.041 ± 0.001	0.997	−24.399 ± 0.001	0.7000 ± 0.0046	0.1258 ± 0.0042	24.123 ± 0.003
308.15	99.229 ± 0.001	1.000	−25.020 ± 0.002	0.8193 ± 0.0055	0.1222 ± 0.0047	24.155 ± 0.003
313.15	100.68 ± 0.000	0.998	−28.068 ± 0.002	0.9723 ± 0.0059	0.1201 ± 0.0054	24.186 ± 0.003
0.001 *m*[a]	**(L- Phe + aqueous MEPN) system**					
298.15	123.460 ± 0.001	0.997	−9.451 ± 0.001	0.8801 ± 0.0017	0.1236 ± 0.0028	34.003 ± 0.003
303.15	126.080 ± 0.000	0.995	−14.292 ± 0.001	1.1115 ± 0.0021	0.1185 ± 0.0026	34.031 ± 0.003
308.15	127.757 ± 0.000	0.999	−18.740 ± 0.000	1.3967 ± 0.0015	0.1159 ± 0.0037	34.077 ± 0.002
313.15	129.587 ± 0.001	0.999	−24.287 ± 0.001	1.5991 ± 0.0038	0.1065 ± 0.0057	34.114 ± 0.004
0.003 *m*[a]	**(L- Phe + aqueous MEPN) system**					
298.15	124.810 ± 0.001	0.997	−12.865 ± 0.001	1.0711 ± 0.0033	0.1215 ± 0.0037	34.009 ± 0.003
303.15	127.537 ± 0.001	0.999	−18.724 ± 0.001	1.2710 ± 0.0047	0.1113 ± 0.0051	34.047 ± 0.002
308.15	129.224 ± 0.001	0.999	−23.057 ± 0.002	1.5523 ± 0.0023	0.1077 ± 0.0048	34.083 ± 0.004
313.15	130.987 ± 0.001	0.998	−28.336 ± 0.000	1.7073 ± 0.0049	0.1036 ± 0.0050	34.127 ± 0.003
0.005 *m*[a]	**(L- Phe + aqueous MEPN) system**					
298.15	126.101 ± 0.001	0.998	−16.196 ± 0.001	1.3426 ± 0.0031	0.1195 ± 0.0042	34.015 ± 0.003
303.15	129.008 ± 0.000	0.999	−23.345 ± 0.002	1.4986 ± 0.0042	0.1089 ± 0.0062	34.054 ± 0.002
308.15	130.697 ± 0.000	1.000	−27.682 ± 0.000	1.6926 ± 0.0051	0.1045 ± 0.0049	34.100 ± 0.003
313.15	132.526 ± 0.001	1.000	−33.047 ± 0.002	1.8544 ± 0.0054	0.0979 ± 0.0062	34.144 ± 0.003

[a] molality (*m*) of aqueous MEPN solution.; Overall standard uncertainty in molality according to the mass purity of the studied samples is to be ±0.0083 mol kg^{-1}.
[b] Standard uncertainties in temperature u(T) = ± 0.01 K; Standard uncertainties in Viscosity u(η) = ± 0.035 mPa; Standard uncertainties in refractive indices u(n_D) = ± 0.0032.

The standard uncertainty in molar conductance *(Λ)* was ±0.05 mS cm^2 mol^{-1}.

Surface tension measurement of the solutions was performed by a Tensiometer machine which is K9, KRUSS; Germany using the technique of platinum ring detachment at $T = 298.15$ K. The uncertainity in surface tension measurement was about in the range ±0.3 mN/m.

The UV spectral pattern was determined by the JASCO V-530 UV-VIS spectrophotometer having the exactness of wavelength ±2 nm. We have fixed the temperature of all measuring solutions using a thermostat.

For recording the ^{1}H NMR spectra, a 400 MHz Bruker ADVANCE DRX machine was applied to analyze the chemical shifts (δ in ppm unit) for protons attached in chemical structures at $T = 298.15$ K in D_2O solvent. The interaction present between the drug and amino acids was analyzed from the recorded differences in chemical shift values (δ) of protons. The uncertainty of the δ value was measured to be superior to 0.0005 ppm.

2.2. Computational information

In our current study, all the necessary DFT estimations were executed with the help of the Gaussian 16 program [18]. B3LYP-D3/6-31+G(d) level of theory has been applied to optimize the geometries of the ground state of composite systems, MEPN, and AA. Dispersion corrected hybrid B3LYP functional reports fairly dependable and accurately expresses the non-covalently bonded interaction energies such as hydrogen bonding, π–π stacking obtainable within the π-system [19]. Following the ground state optimized geometry, time-dependent DFT (TD-DFT) calculations were employed to obtain excited state properties by taking into account lowest 30 singlet excitations [20]. In the optimization process and TD-DFT calculations, solvent effects (water) were incorporated by applying the Polarizable Continuum Model (PCM) [21]. At the identical level of theory, the optimized geometries parallel to minima on the potential energy surfaces were established by vibration frequency (no imaginary frequency) evaluation at the same time [22, 23]. Dissimilar kinds of weak interactions like hydrogen-bonding interaction, van Der Waals force of interaction, and steric repulsion were envisaged by Non-Covalent Interaction (NCI) [24] index plots of the reduced density gradient (RDG *or* s) vs. molecular density ρ have been evaluated through Multiwfn 2.6 [25] suite at the ground state geometries. Maps related to Molecular electrostatic potential

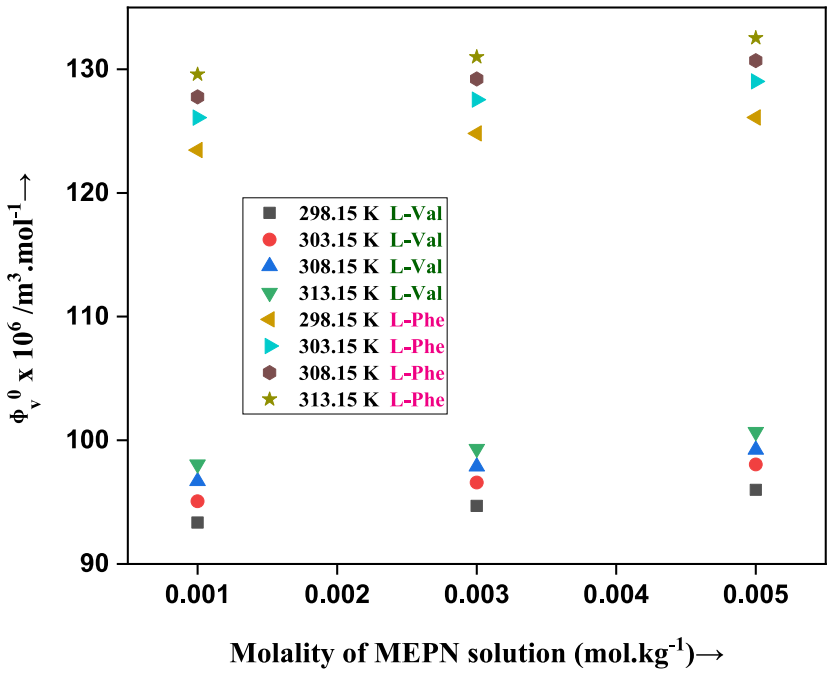

Fig. 1. Plot of Limiting apparent molar volume ($\varphi_V{}^0$) for two different AAs vs. Molality of MEPN in aqueous solution(or concentration)/mol.kg^{-1} with the variation of temperature (in K).

(MESP) have been produced at the identical level of theory to recognize the charge-transfer phenomena between the AA and MEPN [26]. Additionally, the adsorption energies or binding energies (ΔE_{ads}) for those studied composite systems have been assessed by the following expression:

$$\Delta E_{ads} = E_{MEPN-AA} - E_{MEPN} - E_{AA}$$

where $E_{MEPN\text{-}AA}$, $E_{MEPN,}$ and E_{AA} are the total energy of the geometry-optimized composite systems, free MEPN, and the AA molecule, respectively.

3. Results and discussion

The physical properties, like density (ρ) expressed in kg.m^{-3}, viscosity (η) represented in mPa.s unit, and refractive index (n_D), of binary solutions of aqueous MEPN in altered concentrations (0.001 mol kg^{-1}, 0.003 mol kg^{-1}, and 0.005 mol kg^{-1}) at four temperatures i.e, $T = 298.15$ K–313.15 K gapping of 5 K are listed in Table S2.

The experimentally analyzed above physical parameter data of AAs L-Val and L-Phe in the above-mentioned concentrations of MEPN in aqueous solution at four said temperatures are shown in Table S3-Table S5.

3.1. Apparent molar volume

The significant parameters apparent molar volume (φ_V) and another determined term limiting apparent molar volume ($\varphi_V{}^0$) perform an outstanding role in understanding the interactions that happen involving the AAs and aqueous MEPN solutions. φ_V can be articulated from the geometric volume of the inner solute particle in addition to changes in volume for the presence of an aqueous MEPN drug solution around the co-sphere. With the help of the following equation-3, we can determine the φ_V from density values of the mixtures [27], and the outcomes are noted in Table S6-Table S9.

$$\varphi_V = M/\rho - (\rho - \rho_0)/m\rho\rho_0 \quad (3)$$

here M depicts the molar mass of present AA (kg.mol^{-1}), m stands for taken solution's molality (mol.kg^{-1}), ρ and ρ_0 represent the densities of the AAs in aqueous MEPN solution, and aqueous MEPN solvent (kg.m^{-3}) respectively.

The φ_V values become positive and high for every experimental system suggesting the greater solute-solvent interactions and φ_V showing a continuous decrease with a raise in concentration (molality, m) of the taken AAs (L-Phe and L-Val) in a similar concentration of aqueous MEPN solution at the definite temperature (Tables S10–S12). It is also seen that φ_V enhance with rising temperatures and also with the molality of MEPN in an aqueous solution (Tables S10–S12), the variation plotting against $\sqrt{m}$ outcomes to be linear by following the renowned Masson equation [28] which is used to analyze $\varphi_V{}^0$ by least-squares technique. $\varphi_V{}^0$ (partial molar volume

Table 2
Volume transfer/$\Delta_{tr}\Phi_V^0$ for L-Val/L-Phe aqueous solutions of (0.001, 0.003, 0.005) mol.kg^{-1} MEPN at 298.15 K, 303.15 K, 308.15 K, 313.15 K at atmospheric pressure 0.1 mPa.

Temperature/(K)	$\Delta_{tr}\Phi_V^0$ x 10^6/(m^3. mol^{-1}) for L-Val	$\Delta_{tr}\Phi_V^0$ x 10^6/(m^3. mol^{-1}) for L-Phe
0.001 mol kg^{-1} aqueous MEPN 0.001 mol kg^{-1} aqueous MEPN		
298.15 K	−3.067	−3.230
303.15 K	−3.386	−3.410
308.15 K	−3.024	−3.463
313.15 K	−3.165	−3.533
0.003 mol kg^{-1} aqueous MEPN 0.003 mol kg^{-1} aqueous MEPN		
298.15 K	−1.714	−1.880
303.15 K	−1.872	−1.953
308.15 K	−1.843	−1.996
313.15 K	−1.910	−2.133
0.005 mol kg^{-1} aqueous MEPN 0.005 mol kg^{-1} aqueous MEPN		
298.15 K	−0.419	−0.589
303.15 K	−0.398	−0.482
308.15 K	−0.485	−0.523
313.15 K	−0.543	−0.594

referred to at infinite dilution) values are gained from the equation-4 and given in Table 1.

$$\varphi_V = \varphi_V{}^0 + S_V{}^* \sqrt{m} \tag{4}$$

Here $\varphi_V{}^0$ represents the limiting value point of φ_V at the moment of infinite dilution and the term $S_V{}^*$ can be measured from the experimentation slope of the above equation-4, which expresses the solute-solute interaction nature of the solution. Only solvent molecules of MEPN are situated surrounding each solute molecule of amino acids at infinite dilution so $\varphi_V{}^0$ is not show any effect for the interaction arising between the solute particles only and it can only express the interaction that happens in the molecules of solute and solvent.

By the assessment of Table 1 and Fig. 1, it is displayed that $\varphi_V{}^0$ terms showing positive and utmost for L-Phe in 0.005 mol kg^{-1} aqueous MEPN solution at $T = 313.15$ K suggesting greater solute-solvent interaction arises in between L-Phe and aqueous MEPN solution, whereas minimum interaction observes for L-Val in 0.001 mol kg^{-1} aqueous MEPN solution at $T = 298.15$ K giving information that least solute-solvent interaction happens in the middle of L-Val and aqueous MEPN solution. When we compare $\varphi_V{}^0$ with $S_V{}^*$ values, outcomes show that $\varphi_V{}^0$ has a greater magnitude comparison to $S_V{}^*$ for solutions indicating the solute-solvent interactions predominate over the solute-solute interaction for both the observed systems at investigated ($T = 298.15$ K–313.15 K) temperatures. $S_V{}^*$ values are obtaining negative and a continuous decrease is seen if we raise the temperature, it represents that the interaction between the solute AA-solute AA is missing for both systems of AAs in an aqueous MEPN solution.

Co-sphere overlap representation [29] helps to predict that there are three different forms of interactions that exist between AA and MEPN which are categorized as (a) Ion-Dipole interactions occur in presence of $-NH_3^+$ group or $-COO^-$ group of AA(L-Val and L-Phe) and alcoholic –OH part of MEPN; (b) Ion-Hydrophobic interactions present between the $-NH_3^+$ group or COO^- group of both AAs and the hydrophobic parts of MEPN; (c) Hydrophobic-Hydrophobic interactions between the non-polar groups (aromatic and alkyl part) of MEPN and hydrophobic zone present in the AA. On comparing the structural context, for both the amino acids, all these interactions are highly efficient in L-Phe comparison to L-Val because there is a presence of a larger hydrophobic non-polar aromatic benzene ring that can be authenticated afterward by the assistance of computational studies.

The deviation of $\varphi_V{}^0$ with altering temperature observed from $T = 298.15$ K–313.15 K suitably follows this polynomial equation-5:

$$\varphi_V{}^0 = a_0 + a_1 T + a_2 T^2 \tag{5}$$

In this equation-5, a_0, a_1, and a_2 these three-term expressed as the empirical coefficients, and the terms are calculated by utilizing least-squares fitting of $\varphi_V{}^0$ with changing temperatures, which depend on the characteristics of the solute particle and the molality (m) of aqueous MEPN solution and T representing temperature that expressed in Kelvin unit. In Table S6, the Coefficient terms of equation-5 for AAs L-Val and L-Phe in various concentrations of MEPN in aqueous solution are listed.

The following numerical expression equation-6 is used to achieve limiting apparent molar expansibility term, $\varphi_E{}^0$ for various temperatures.

$$\varphi_E{}^0 = \left(\delta\varphi_V{}^0/\delta T\right)_P = a_1 + 2a_2 T \tag{6}$$

If we are differentiating equation-5 with respect to temperature, then we get $\varphi_E{}^0$ values. The following thermodynamic expression (Equation-7) given by Hepler is used to obtain the value of $(\delta\varphi_E^0/\delta T)_P$ which can recommend the prolonged structure-making or breaking ability of the solute AA in the aqueous MEPN medium by considering its sign [30].

$$\left(\delta\varphi_E{}^0/\delta T\right)_P = \left(\delta^2\varphi_V{}^0/\delta T^2\right)_P = 2a_2 \tag{7}$$

A negative sign $(\delta\varphi_E{}^0/\delta T)_P$ means structure-breaking; otherwise, the positive value $(\delta\varphi_E{}^0/\delta T)_P$ suggests structure-making [31].

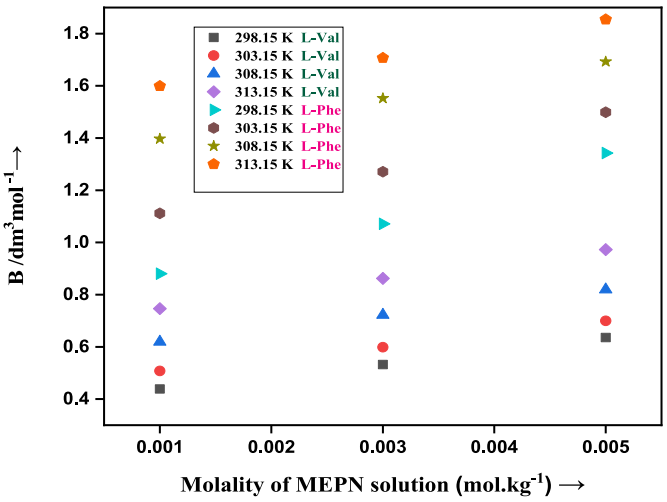

Fig. 2. Viscosity B-Coefficient of two individual AAs vs. Change in molality of aqueous MEPN(or concentration)/mol.kg^{-1} at altered temperatures (in K).

According to Table S7, $(\delta\varphi_E{}^0/\delta T)_p$ have negative values for both the AAs in the aqueous MEPN system. After analysis of our investigation, we have found the outcomes that the selected AAs (solutes) show the structure-breaker property for all concentrations of the aqueous MEPN solutions and the tendency increases with increasing the concentration of MEPN in aqueous solution. Therefore we can conclude that the solvent structure is interrupted by the surrounding environment of AAs because of the enhancement of the interactions in the presence of solute and solvent molecules.

Transfer volume measurements:

Using Equation-3, the φ_V values of the AAs (L-Val and L-Phe) in aqueous medium were calculated from the density values. φ_V^0 were also determined from the φ_V of the AAs. Without taking into account the interactions effects of solute-solvent, it is possible to describe both qualitative and quantitative information about the interactions relating solute-solvent based on limiting apparent molar volume of transfer [32]. With the use of the following relation, the transfer volume $\Delta_{tr}\varphi_V^0$ of L-Val/L-Phe from water to aqueous MEPN solutions was calculated.

$$\Delta_{tr}\,\varphi_V{}^0 = \varphi_V{}^0{}_{MEPN\ aq.sol\text{n.}} - \varphi_V{}^0{}_{aq.sol\text{n}}$$

where $\varphi_{V\,aq.soln.}^0$ is the limiting apparent molar volume of AA in water listed in Table S18 and the $\Delta_{tr}\varphi_V^0$, values for L-Val/L-Phe in H_2O to aqueous MEPN solutions are shown in Table 2.

The values of φ_V^0 of L-Val/L-Phe given in aqueous MEPN solution were found to be smaller than those of the L-Val/L-Phe in water. It was found from the listed table that the $\Delta_{tr}\varphi_V^0$, values all are negative for both L-Val and L-Phe in aqueous MEPN solution. In general, there are three interactions pattern occurring between L-Val/L-Phe and aqueous MEPN solution, can be categorized as follows:

(i) Ion-Dipole interactions occur in presence of $-NH_3^+$ group or COO^- group of L-Val/L-Phe and alcoholic –OH part of MEPN.
(ii) Ion-Hydrophobic interactions occur in between the $-NH_3^+$ group or COO^- group of both AAs and the hydrophobic parts of MEPN.
(iii) Hydrophobic-Hydrophobic interactions between the aromatic and alkyl part of MEPN and hydrophobic part of L-Val/L-Phe.

While the negative contribution to $\Delta_{tr}\varphi_V^0$ value indicates that the interaction types will be ion-hydrophobic and hydrophobic-hydrophobic, which cause by disrupting the side group by the negative ending part, the positive contribution to $\Delta_{tr}\varphi_V^0$value indicates that the interaction types will be ion-ion, which causes reduction of electrostriction at the terminal end. The results of our current investigation show that $\Delta_{tr}\varphi_V^0$ is negative for both L-Val and L-Phe in aqueous MEPN solution for concentrations (0.001, 0.003, 0.005) mol.kg^{-1} and working temperatures (293.15, 298.15, 303.15, 308.15, 313.15) K. So the aforementioned $\Delta_{tr}\varphi_V^0$ results lead to the conclusion that ion-hydrophobic and hydrophobic-hydrophobic interactions (ii) and (iii) dominate the Ion-Dipole interactions (i) in these cases.

3.2. Viscosity

The viscometric study facilitates dealing with the configuration and interactions due to molecular assembly present in the solution. The determined experimental viscosities are recorded for the investigated sets in Table S3-Table S5. The following Jones-Dole equation-8 is utilized for the evaluation of relative viscosity (η_r) [33].

Table 3
Values of $(\overline{V_1}^0 - \overline{V_2}^0)$, $\Delta\mu_1^{0\neq}$, $\Delta\mu_2^{0\neq}$, $T\,\Delta S_2^{0\neq}$, and $\Delta H_2^{0\neq}$ for L-Val and L-Phe in altered concentrations of MEPN in aqueous solution at changing temperatures.

Concentrations of MEPN in aqueous solution (mol • kg^{-1})	L-Valine				
	Parameters				
	$(\overline{V_1}^0 - \overline{V_2}^0)$/m^3. mol^{-1}	$\Delta\mu_1^{0\neq}$/kJ. mol^{-1}	$\Delta\mu_2^{0\neq}$/kJ. mol^{-1}	$T\Delta S_2^{0\neq}$/kJ. mol^{-1}	$\Delta H_2^{0\neq}$/kJ. mol^{-1}
$T = 298.15$ K					
0.001	−75.09	9.13	78.91	−945.55	−866.64
0.003	−76.08	9.20	90.20	−1004.71	−914.51
0.005	−77.01	9.26	102.37	−1009.39	−907.02
$T = 303.15$ K					
0.001	−76.78	8.97	89.57	−961.41	−871.84
0.003	−77.93	9.07	100.59	−1021.55	−920.97
0.005	−79.04	9.17	112.49	−1026.31	−913.83
$T = 308.15$ K					
0.001	−78.38	8.87	106.50	−977.27	−870.77
0.003	−79.20	8.98	118.98	−1038.40	−919.43
0.005	−80.19	9.08	130.15	−1043.24	−913.10
$T = 313.15$ K					
0.001	−79.72	8.82	126.12	−993.12	−867.00
0.003	−80.61	8.94	140.23	−1055.25	−915.02
0.005	−81.61	9.02	152.91	−1060.17	−907.26
Concentrations of MEPN in aqueous solution (mol • kg^{-1})	L-Phenylalanine				
	Parameters				
	$(\overline{V_1}^0 - \overline{V_2}^0)$/m^3. mol^{-1}	$\Delta\mu_1^{0\neq}$/kJ. mol^{-1}	$\Delta\mu_2^{0\neq}$/kJ. mol^{-1}	$T\Delta S_2^{0\neq}$/kJ. mol^{-1}	$\Delta H_2^{0\neq}$/kJ. mol^{-1}
$T = 298.15$ K					
0.001	−105.21	9.13	142.95	−2198.11	−2055.16
0.003	−106.20	9.20	165.98	−1969.31	−1803.33
0.005	−107.12	9.26	198.62	−1589.77	−1391.14
$T = 303.15$ K					
0.001	−107.80	8.97	177.12	−2234.97	−2057.85
0.003	−108.90	9.07	195.65	−2002.34	−1806.68
0.005	−110.01	9.17	222.51	−1616.43	−1393.92
$T = 308.15$ K					
0.001	−109.45	8.87	219.67	−2271.84	−2052.17
0.003	−110.55	8.98	237.16	−2035.36	−1798.20
0.005	−111.67	9.08	251.92	−1643.09	−1391.17
$T = 313.15$ K					
0.001	−111.25	8.82	251.65	−2308.70	−2057.05
0.003	−112.29	8.94	262.23	−2068.39	−1806.16
0.005	−113.46	9.02	277.69	−1669.75	−1392.06

molality (m) of aqueous MEPN solution; Overall standard uncertainty in molality according to the mass purity of the studied samples is to be ±0.0083 mol kg^{-1}; Standard uncertainties in temperature u(T) = ± 0.01 K.

$$(\eta / \eta_0 - 1) / \sqrt{m} = (\eta_r - 1) / \sqrt{m} = A + B\sqrt{m} \tag{8}$$

Here $\eta_r = \eta/\eta_0$ suggests the relative viscosity value for the solution, where η and η_0 represent the viscosities of ternary mixtures of AAs in aqueous MEPN solution and solvent aqueous MEPN respectively and m depicts the molality of AAs in aqueous MEPN solutions. In mathematical expression (equation-8), the Falkenhagen coefficient is expressed as the term A [34]. Applying ionic attraction theory given by Falkenhagen-Vernon, the term A is calculated which indicates the solute-solute interaction and the Jones-Dole co-efficient, term B, also known as viscosity B-coefficients, gives knowledge for interactions that occur between solute and solvent molecules exist in solution medium due to inducement of structural modifications. Viscosity A- and B- coefficients are determined using the least-square method when $(\eta_r - 1)/\sqrt{m}$ plotted against $\sqrt{m}$ and the obtained results are shown in Table 1. According to the inspection of Table 1, A-coefficient terms diminish with an enhancement of temperature for the individual taken AAs. From the outcomes, we recommend that a very weak solute-solute (AA-AA) interaction exists in an observed medium that demonstrates similar conformity with those calculated values S_V^*.

From the viscosity B-coefficient term [35], we acquire precious concepts on the topic of the solvation of solvated AAs and its control of the solvent structure arrangement by surrounding AAs in solutions. According to Table 1 and Fig. 2, the B-coefficients come positive and show greater outcomes in comparison to A-coefficients, providing the idea that the solute-solvent interaction predominates over the solute and solute (AA-AA) interaction. The positive values of the term viscosity B-coefficient are raised with enhancing temperature and molality of aqueous MEPN solution which gives information that the interaction arising between solute and solvent molecules enhances with raising the temperature and also with the concentration of MEPN in aqueous solution. Viscosity B-coefficient values of

L-Phe in aqueous MEPN solution are higher than L-Val in aqueous MEPN solution indicating greater solute-solvent interaction prevails in L-Phe in aqueous MEPN solution. The conclusions made from these are nicely supported by those investigated using ${\varphi_V}^0$ values.

If the *B*-coefficient has a Positive value, that means kosmotropes which are strongly and tightly hydrated molecules of solute display a larger alter in viscosity parameters with changing concentration whereas the negative term gives the idea of chaotropes for hydrated solute molecules which have feeble and weak nature [36]. The *B*-coefficients may perhaps not be properly supported, remarkably for AAs having big hydrophobic groups. The higher outcomes of $B/\ {\varphi_V}^0$ suggest the primary solvation shell [37]. The $B/\ {\varphi_V}^0$ has a value of 0–2.5 depicting unsolvated spherical species [38]. The structure-making or breaking capability of solute(AA) is better expressed by the *dB/dT* ratio more willingly than the sign or magnitude of the Viscosity *B*-coefficient [39]. The negative outcomes of *dB/dT* recommend a structure-making (kosmotropic) nature and the positive outcomes of *dB/dT* show a structure-breaking (chaotropic) property of AAs in drug solutions respectively. From Eyring's theory of viscosity [40], the *dB/dT* concept arises which represents that a negative value of this term expresses higher activation energy for the viscous flow of solution in comparison with aqueous MEPN solvent.

From the inspection of Table S8 and Table S9, the *B*-coefficient values are increasing with temperature for both amino acids i.e. positive values of *dB/dT*. Higher values of $B/\ {\varphi_V}^0$ represent the creation of a primary solvation shell and positive *dB/dT* values indicate both amino acids L-Val and L-Phe are classified as structure-breakers in an aqueous MEPN solution.

With the assistance of Eyring and workmates [41], the term ${\Delta\mu_1}^{0\neq}$, free activation energy expression per mole solvent for the viscous flow is determined using the following equation-9:

$$\eta_0 = \left(hN_A \,/\, \overline{V_1}^0\right)\exp\left({\Delta\mu_1}^{0\neq} \,/\, RT\right) \tag{9}$$

Here *h* is Planck's constant, N_A is Avogadro's number and the partial molar volume of aqueous MEPN solvent is represented by $\overline{V_1}^0$. Equation-9 can also be mentioned as follows:

$${\Delta\mu_1}^{0\neq} = RT\ln\left(\eta_0 \overline{V_1}^0 \,/\, hN_A\right) \tag{10}$$

According to Feakins et al. [42–44], by solving both equations-8 and -10, we get

$$B = \left(\overline{V_1}^0 - \overline{V_2}^0\right) + \overline{V_1}^0\left[\left({\Delta\mu_1}^{0\neq} - {\Delta\mu_2}^{0\neq}\right) \,/\, RT\right] \tag{11}$$

where $\overline{V_2}^0$ express limiting partial molar volume (${\varphi_V}^0$) of the solute AAs and at infinite dilution condition, ionic activation energy term is denoted per mole of AA by ${\Delta\mu_2}^{0\neq}$. By rearranging equation-11, equation-12 find as,

$${\Delta\mu_2}^{0\neq} = {\Delta\mu_1}^{0\neq} + \left(RT \,/\, \overline{V_1}^0\right)\left[B - \left(\overline{V_1}^0 - \overline{V_2}^0\right)\right] \tag{12}$$

By the inspection of Table 3, the ${\Delta\mu_2}^{0\neq}$ results are positive and much higher than ${\Delta\mu_1}^{0\neq}$, representing that the existing interaction between the AA solutes and aqueous MEPN solvent is very much stronger in the Ground State (G.S.) rather than the Transition State (T.S.). The solvation of the solute is not favorable in the T.S. following free energy.

The entropy of activation ${\Delta S_2}^{0\neq}$ [41] of experimental solutions is derived by using the following equation-13,

$${\Delta S_2}^{0\neq} = -d\left({\Delta\mu_2}^{0\neq}\right) \,/\, dT \tag{13}$$

when ${\Delta\mu_2}^{0\neq}$ plots against *T*, then the slope value ${\Delta S_2}^{0\neq}$ has been determined using a least-squares method.

Then ${\Delta H_2}^{0\neq}$ enthalpy of activation [45] has been evaluated using the following relation (equation-14):

$${\Delta H_2}^{0\neq} = {\Delta\mu_2}^{0\neq} + T{\Delta S_2}^{0\neq} \tag{14}$$

The values of ${\Delta S_2}^{0\neq}$ and ${\Delta H_2}^{0\neq}$ from equation-14, are recorded and mentioned in Table 3 as a reference.

Considering Tables 3 and it is obvious that the ${\Delta\mu_1}^{0\neq}$ values are fundamentally constant for all the concentrations (molality) of the MEPN in aqueous solution, which proves that the dependence of ${\Delta\mu_2}^{0\neq}$ mainly based on the viscosity coefficients and $(\overline{V_1}^0 - \overline{V_2}^0)$ terms. The ${\Delta\mu_2}^{0\neq}$ values are Positive at the investigated temperatures (T = 298.15 K–313.15 K) and solvent aqueous MEPN compositions inspected suggesting that the viscous flow phase becomes more complicated as the temperature and molality of the aqueous MEPN solution increase. According to outcomes, the T.S. appearance turns out to be less important. Feakins et al. propose that [46,47] if a substance has + ve *B*-coefficients and ${\Delta\mu_2}^{0\neq} > {\Delta\mu_1}^{0\neq}$ that means stronger solute-solvent interactions i.e., the T.S. formation is allowed by breaking the intermolecular forces in the aqueous MEPN solvent structure in the system [37,39,48]. The negative values of ${\Delta S_2}^{0\neq}$ and ${\Delta H_2}^{0\neq}$ recommending that the T.S. formation is related to bond-making and enhancing in order. Nonetheless, the exact mechanism for the framework is complicated to build up for this, though the chaotic condition may be suggested for the slip-plane [37, 49,42]. Following the proposal of Feakins et al. model, both AAs show ${\Delta\mu_2}^{0\neq} > {\Delta\mu_1}^{0\neq}$, so they act as structure-breakers in the aqueous MEPN solution. The *dB/dT* value for both the solutes in the aqueous MEPN solution is well supported by these thermodynamic data shown in Table 3.

3.3. Refractive index

The refractive index (n_D) measurement is a significant characteristic of finding out the interactions of molecular assembly that appear in the environment of the solution. The following equation-15 is known as the Lorentz-Lorenz equation which is utilized to

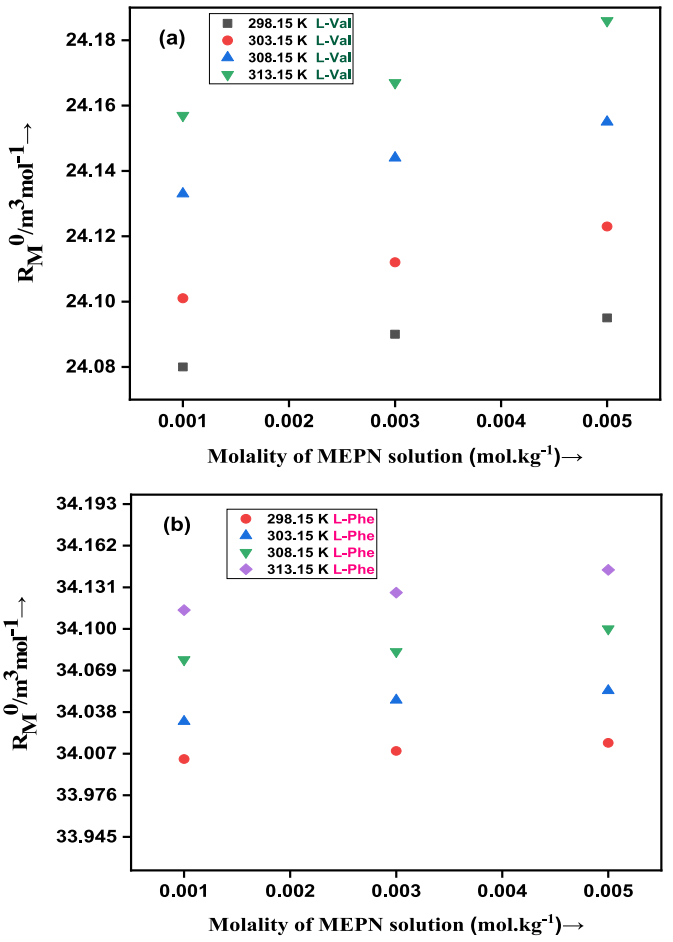

Fig. 3. Change of limiting molar refraction (Rᴍ°) vs. altered molality of MEPN in aqueous solution (or concentration)/mol.kg^{-1} with the variation of temperatures (in K).

estimate the molar refraction (R_M) [43].

$$R_M = \{(n_D{}^2 - 1) / (n_D{}^2 + 2)\}(M / \rho) \tag{15}$$

here R_M, n_D recommend the molar refraction and refractive index value of the solution respectively. The n_D of a substance is stated by the ratio c_o/c, where c and c_o implied the light's velocity in the case of definite medium and the vacuum respectively. The substance that possesses a higher value of the refractive index is highly capable of refracting light effortlessly because these values describe its potential for any compound when the light's refraction starts from one medium and passes into another medium [44]. Deetlefs et al. [50] proposed that the substance containing closely packed and denser molecules have a greater magnitude of refractive index. After a check-up of Table S3-Table S5 and Table S10-Table S12, it can be recommended that the refractive index and molar refraction both are greater for the selected L-Phe than L-Val in different concentrations of MEPN in aqueous solution, signifying that the molecules are more closely bound in the (L-Phe + aqueous MEPN) system.

Limiting molar refraction (R_M^0) is evaluated by the application of this numerical expression-16 and the outcomes are enlisted in Table 1.

$$R_M = R_M{}^0 + R_S\sqrt{m} \tag{16}$$

According to Table 1 and Fig. 3, it is seen that the R_M^0 values rise with the enhancing temperature and also with the concentration (molality) of the MEPN in an aqueous solution, demonstrating that the interaction arises in solute and solvent molecules, is developed with the enhancement in temperature and molality of aqueous MEPN solution. The R_M^0-values of L-Phe in the aqueous MEPN solution are well greater in comparison to L-Val in all respects, communicating that a better solute-solvent interaction prevails in between L-Phe and aqueous MEPN system respectively. These discoveries are also similarly verified with the results of $\varphi_V{}^0$ and viscosity B-coefficients that were justified earlier.

Table 4
Limiting Slopes ($\partial\sigma/\partial m$) of surface tension of AAs selected in the aqueous MEPN solutions.

Concentrations of MEPN in aqueous solution (mol • kg^{-1})	($\partial\sigma/\partial m$)/mN.m^{-1}.kg. mol^{-1}	
	L-Val + aqueous MEPN	L-Phe + aqueous MEPN
0.001	−71.357 ± 0.229	−92.897 ± 0.189
0.003	−85.327 ± 0.103	−105.674 ± 0.250
0.005	−102.243 ± 0.217	−134.381 ± 0.130

molality (m) of aqueous MEPN solution; Overall standard uncertainty in molality according to the mass purity of the studied samples is to be ±0.0083 mol kg^{-1}; Standard uncertainties in temperature u(T) = ± 0.01 K and Standard uncertainties in surface tension u(σ) ±0.3 mN/m.

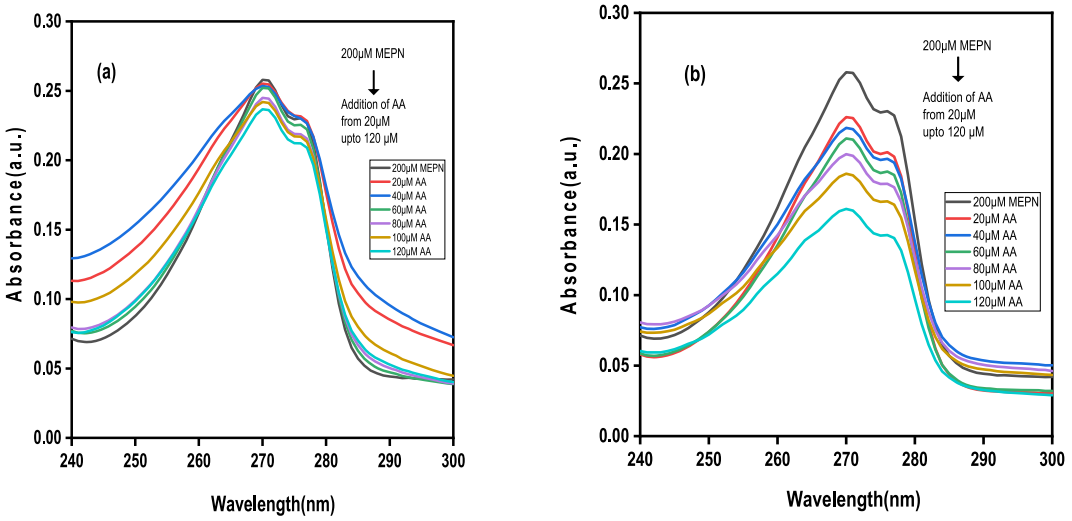

Fig. 4. Double reciprocal plot is shown according to Benesi-Hildebrand for (a) MEPN + L-Val and (b) MEPN + L-Phe system.

3.4. Conductance study

A conductometric study is very much useful for looking at the transportation behaviour happening in the solution media. The conductance study was done for two AAs (L-Val and L-Phe) in aqueous MEPN solutions at four different temperatures (298.15 K, 303.15 K, 308.15 K, 313.15 K). The advantages of this study are to ascertain the interactions (solute-solvent and solute-solvent) and the transportation phenomenon of L-Val and L-Phe in aqueous MEPN solution [51]. The molar conductivities [52] (Λ) of aqueous MEPN solution are detected by raising the concentration of L-Val and L-Phe at four altered temperatures and reported in Table S13. The increase in molar conductivity (Λ) values is observed with a temperature rise and also with enhancing the concentration of aqueous MEPN solution, and the continuous decrease in molar conductivity (Λ) of the solution causes due to the continuous addition of L-Val, and L-Phe in aqueous MEPN solution (Figs. S1–S4). Though the number of ionic species increases in the solution medium after the addition of AAs, L-Val and L-Phe in the aqueous MEPN solution, the molar conductivity diminishes [53]. That may be attributed on account of the enlargement power of solute-solvent interactions between solute and solvent molecules AAs (L-Val or L-Phe) and aqueous MEPN, which are dominated by ion-dipole, dipole-dipole, and hydrophobic-hydrophobic interactions. Due to solute-solvent interactions, the development of molecular gathering increases on increasing the strength of solute-solvent interaction, resulting in the ionic form of solutes mislays their ability to move freely, ultimately showing less mobility so they possess less conductivity in a solution medium. Therefore the study of conductance analysis strongly assists the above volumetric, viscometric, and refractrometric studies and assures similar predictions.

3.5. Surface tension

The experimentation results of surface tension of aqueous MEPN solution and AAs are carried out at $T = 298.15$ K and reported in Table S14. Figs. S5 and S6 depict the changing surface tension of L-Val and L-Phe in an aqueous MEPN solution with the concentration (molality) at $T = 298.15$ K. A rapid decrease is seen in the case of surface tension when we are enhancing the concentration of both AAs L-Val and L-Phe.

From the plot of surface tension values of AAs in aqueous MEPN solution with different concentrations (molality) of the selected experimental solutions, the sign and magnitude can be obtained for limiting slope values indicating the hydrophobic or hydrophilic nature of the AAs, as it portrays the better quality of interaction above the exterior [54,23]. From the very dilute range, the limiting slopes were determined by mean values, and these results are mentioned below in Table 4.

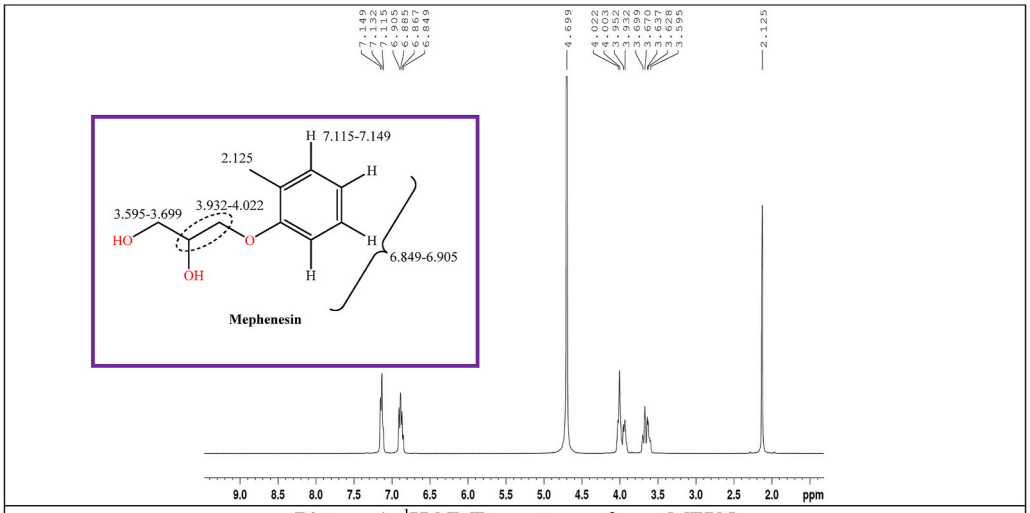

Picture 1: ^{1}H-NMR spectrum of pure MEPN

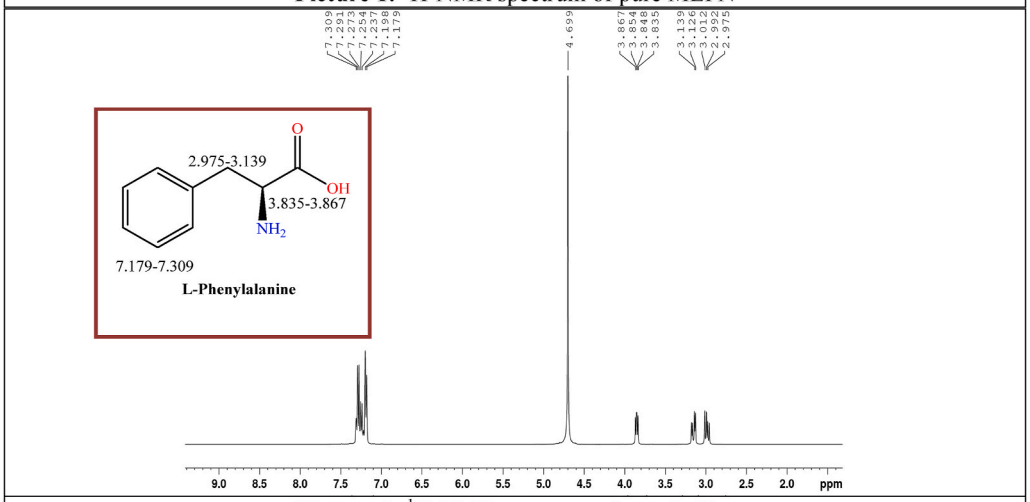

Picture 2: ^{1}H-NMR spectrum of pure L-Phe

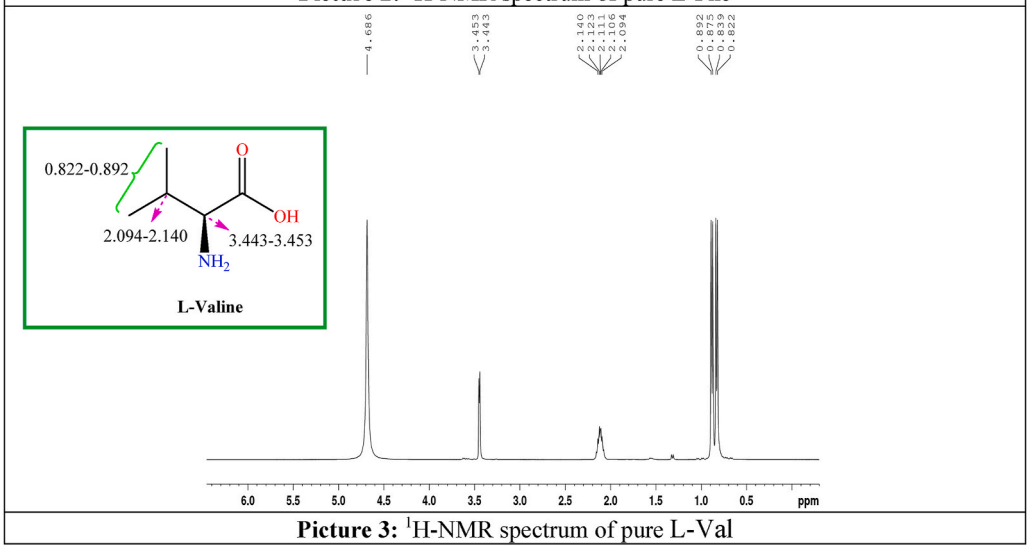

Picture 3: ^{1}H-NMR spectrum of pure L-Val

Fig. 5. Proton NMR spectra of pure MEPN (Pic. 1), L-Phe (Pic. 2), and L-Val (Pic. 3) in D_2O.

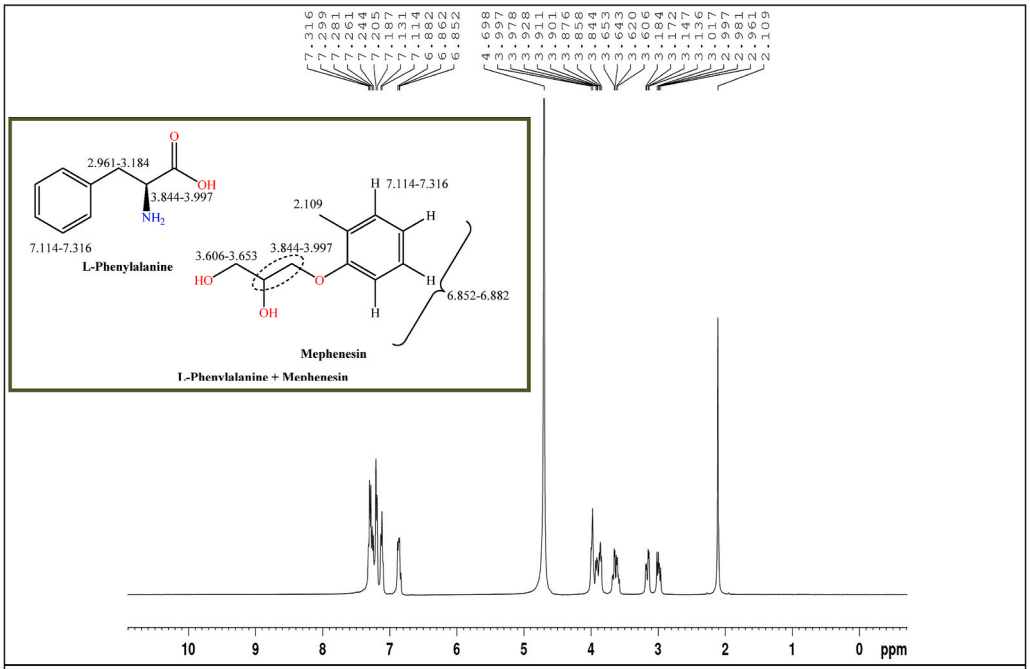

Picture 4: ^{1}H-NMR Spectrum of MEPN + L-Phe

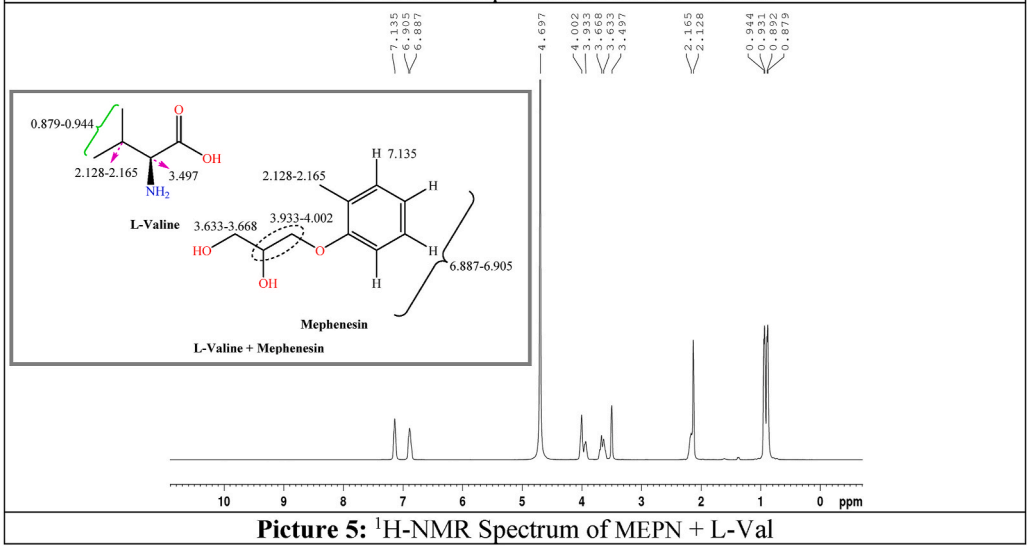

Picture 5: ^{1}H-NMR Spectrum of MEPN + L-Val

Fig. 6. Proton NMR spectra of MEPN + L-Phe (Pic. 4) and MEPN + L-Val (Pic. 5) in D_2O.

The negative sign of $(\partial\sigma/\partial m)$ [53,55] for L-Val and L-Phe in aqueous MEPN solutions gives a concept of surface-active solutes or compounds of hydrophobic nature. This result implies that the hydrophobic side chain influence is more dominant for L-Phe than L-Val so L-Phe can readily show movement to the boundary of liquid and air at which place absorption can be possible.

3.6. UV–visible spectra measurement

UV–Vis absorption learning is used to survey the structural transform and the environment of interactions of the solute AAs with the solvent-aqueous MEPN by gathering information about the stable form of the molecular union by evaluating the association constants (K_a) or stability constant [54]. The learning of such interactions for the different solutions is proven by varying concentrations L-Val/L-Phe in absorbance (A) of MEPN at $\lambda_{max} = 270$ nm (Fig. 4) at $T = 298.15$ K to find out the association constant (Tables S15 and S16). The association constant (K_a) for the system (MEPN + L-Val) and (MEPN + L-Phe) are calculated from the double reciprocal plots [Fig. 4 (a, b)] [23] utilizing the equation given by Benesi-Hildebrand, the plot is linear according to the equation-17, which usually provides the idea of solute-solvent ratio in the mixture [55].

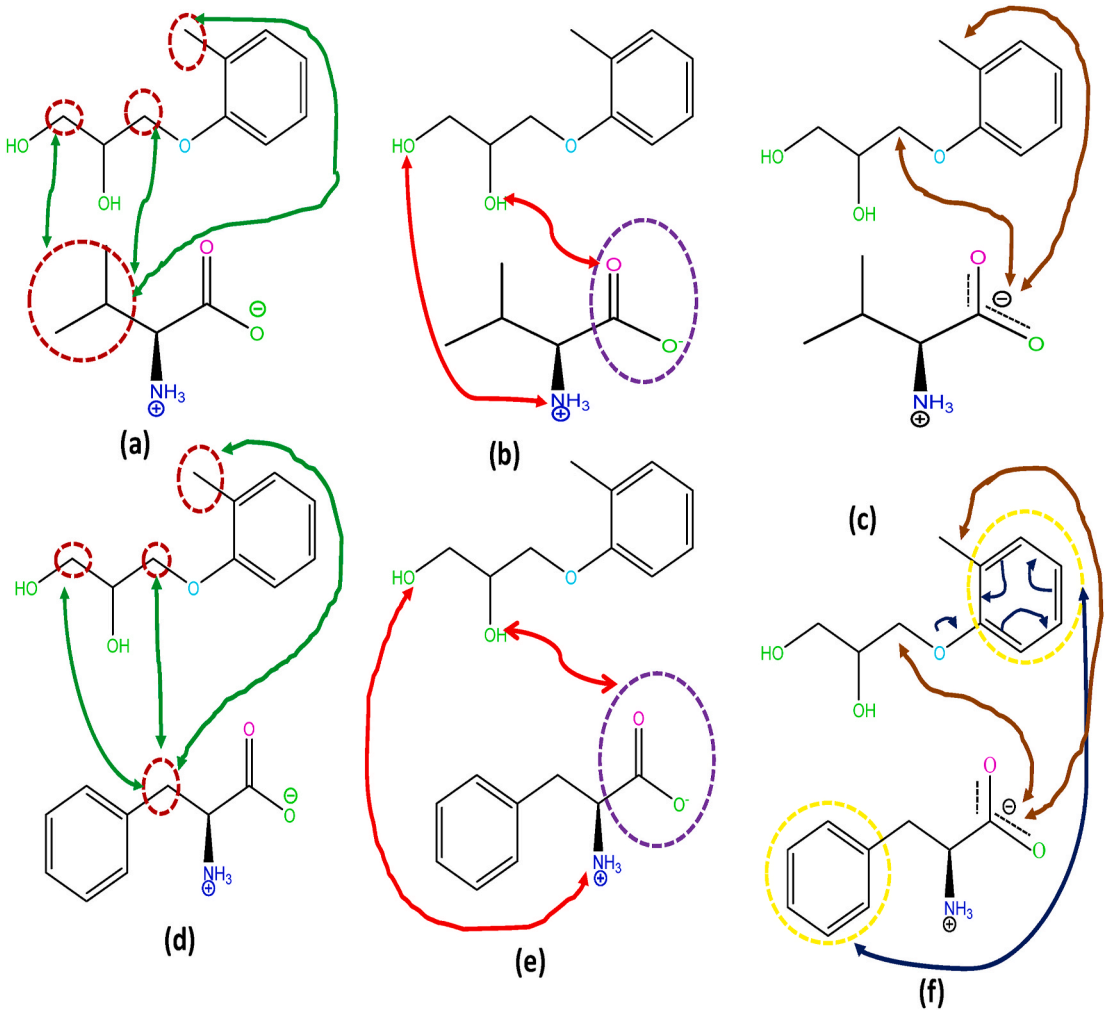

Scheme 2. Plausible sketches of various patterns shown for molecular interactions associate with MEPN drug in presence of two AAs L-Val and L-Phenylalanine: **(a)** and **(d)** Hydrophobic–Hydrophobic interactions ( ); **(b)** and **(e)** Ion-Dipole interaction( ); **(c)** and **(f)** Ion-Hydrophobic interactions ( ) as well as π-π interaction ( ) in case only **(f)**.

$$\frac{1}{\Delta A} = \frac{1}{\Delta\varepsilon[\mathrm{MEPN}]K_a}\frac{1}{[\mathrm{AA}]} + \frac{1}{\Delta\varepsilon[\mathrm{MEPN}]} \tag{17}$$

Where [MEPN] and [AA] depict the total concentration of the MEPN and AAs (L-Val and L-Phe) respectively, $\Delta\varepsilon$ denotes the change of molar extinction co-efficient before the addition and after mixing of AAs with the drug MEPN and ΔA means the absorption changes of MEPN after adding up of AAs. The values of K_a for each of the sets are found from the intercept/slope of the plots [Fig. 4(a and b)] using equation-17. The K_a outcome for (MEPN + L-Val) is 474.593 M^{-1} whereas for (MEPN + L-Phe) is 23243.769 M^{-1} [56].

3.7. NMR data

The ^{1}H NMR spectroscopy [55,57] is deployed to make clear the shifts in the electronic environment of different protons of MEPN in existence of AAs. The chemical shifts of protons of MEPN in D_2O are shown in Picture 1 of Fig. 5. The chemical shifts of diverse protons of L-Phe and L-Val in D_2O are expressed in Pic. 2 and 3 of Fig. 5.

Depending on the adjacent proximity of a compound, there is a change observed in the chemical shift for the environment of protons, all these spectra are shown in the above figures. The chemical shift changes for MEPN and AAs in two different systems of 1:1 (L-Val + MEPN) and (L-Phe + MEPN) are explained in Fig. 6. The δ values shift downfield (higher frequency) or upfield (lower frequency) can be predicted depending on the effects of the surrounding group's deshielding and shielding nature.

The results illustrate that considerable chemical shifts are observed for protons of both MEPN and AAs. The chemical shift changes are developed because of different interaction factors such as ion-dipole, ion-hydrophobic, and hydrophobic-hydrophobic interactions prevailing hugely for suitable parts of MEPN and AAs. This study further emphasizes the previous conclusions obtained from the above

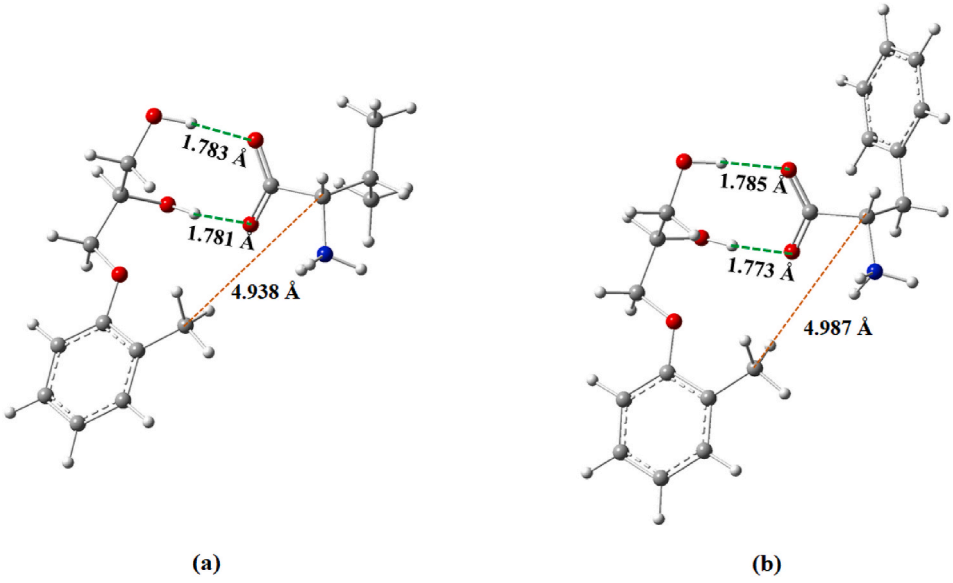

Fig. 7. Optimized geometries regarding the (a) L-Val-MEPN (b) L-Phe-MEPN composite systems.

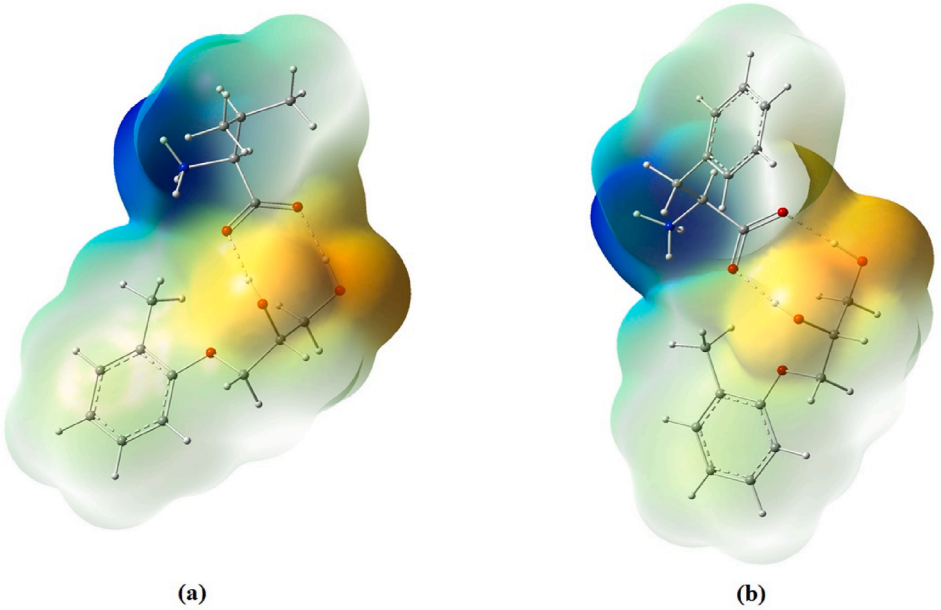

Fig. 8. Electrostatic potential maps regarding (a) L-Val-MEPN (b) L-Phe-MEPN composite system.

physicochemical studies. All types of interactions are represented in Scheme 2.

3.8. Computational study

Optimized geometries drawn for L-Val-MEPN and L-Phe-MEPN composite systems are presented in Fig. 7 (a, b). The high adsorption or binding energy (E_{ads}) of the said composite systems reveals the strong interaction present between the AA (solute) and MEPN (solvent). The calculated E_{ads} of L-Val-MEPN (−162.49 kJ/mol) is smaller compared to that of the L-Phe-MEPN composite systems (−169.93 kJ/mol). These strong interactions in composite systems are attributed due to the occurrence of strong H-bonding interaction involving the positive pole of MEPN with the negative pole of an AA (oxygens of an acid group -COOH) specified by the green line (———) and hydrophobic-hydrophobic interaction occur in presence of hydrophobic part of AA and MEPN indicated by orange line (———) in Fig. 7 (a, b). It is found from Fig. 7 (a, b) that the H-bonding distances (very short) and hydrophobic interaction

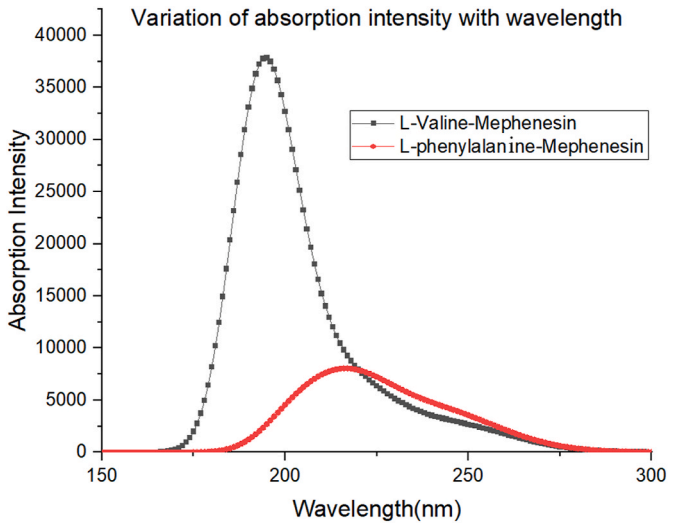

Fig. 9. Simulated absorption spectra (a) L-Val-MEPN (b) L-Phe-MEPN composite system.

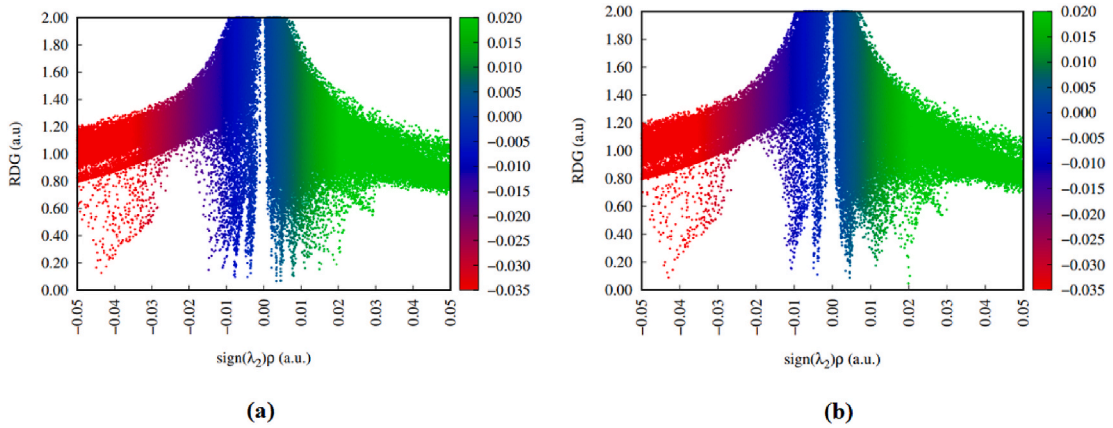

Fig. 10. Plots of reduced density gradient (RDG) against electron density multiplied with a sign of the second Hessian eigenvalue (sign(λ2)ρ(r)) regarding (a) L-Val-MEPN (b) L-Phe-MEPN composite systems.

distances are in similar regions for almost the same in both cases.

Analysis of Molecular electrostatic maps (ESP), as presented in Fig. 8 (a, b) is a very reliable approach to identify the electrostatic type and hydrophobic interactions that occur in AA and MEPN. The yellowish-red areas of ESP maps for both composite systems are very noticeable, indicating that the strong electrostatic interaction between the positive pole of MEPN and the negative pole of an AA (oxygens of –COOH group) is operating. It is found from Fig. 8 (a, b) that the yellowish-red region of the L-Phe-MEPN composite system is more prominent than that of L-Val-MEPN which gives the idea of powerful electrostatic interaction arising in the former.

Furthermore, to obtain theoretical absorption spectra of the L-Val-MEPN, and L-Phe-MEPN composites we have performed TD-DFT calculations as shown in Fig. 9 (a, b). Absorption spectra of L-Val-MEPN showed three peaks (194 nm, Oscillator Strength = 0.3025; 222 nm, Oscillator Strength = 0.0907; 249 nm, Oscillator Strength = 0.0554) while L-Phe-MEPN showed two peaks (222 nm, Oscillator Strength = 0.0959; 249 nm, Oscillator Strength = 0.056) From the simulated absorption spectra of the composite systems it is clear that compared to L-Val-MEPN, absorption maxima of L-Phe-MEPN is slightly red-shifted with reduced intensity. Here we note that our simulated absorption maxima are slightly lower compared to the experimental absorption spectra.

To recognize the weak interactions like hydrogen-bonding interaction, van der Waals, and steric repulsion present in AA-MEPN composite systems, we now have studied the RDG plots [55,58] which are explained in Fig. 10 (a, b). The strong attractive forces have originated such as hydrogen-bonding (red region) and hydrophobic interactions (blue region) are operating between AA and MEPN in both composite systems but the bigger scattered portion of the negative zone connected with RDG plots is watched in the area of L-Phe-MEPN composite system in comparison to L-Val-MEPN composite systems in Fig. 10 (a, b) indicating the presence of stronger attraction force in the former than that in latter. It is also observed in Fig. 10 (a, b) that the repulsive steric interaction is greater (more scattered Green region) for the L-Val-MEPN composite system which is responsible for inhibiting the stable conformation of the said

composite system.

All the above facts confirm that a stronger interaction is occurring for L-Phe-MEPN, these theoretical opinions strengthen the experimental outcomes.

4. Conclusion

The detailed calculations of different thermodynamic parameters and limiting apparent molar volume, limiting molar refraction, viscosity-*B* co-efficient, and molar conductance values at three individual concentrations and four above-mentioned temperatures are very useful to predict that the solute-solvent interaction predominates over solute-solute interaction and varies with concentration and as well as temperature for both the systems and the extent of solvation is highest in L-Phe in 0.005 *m* aqueous MEPN at $T = 313.15$ K and lowest in L-Val in 0.001 *m* aqueous MEPN at $T = 298.15$ K. A positive dB/dT value for both cases shows the structure-breaking behaviour of AAs in aqueous MEPN solution. Surface tension study suggests that the hydrophobic side chain is more influencing for L-Phe in comparison to L-Val in aqueous MEPN solution. The binding constant value for the association of L-Phe-MEPN is higher than the L-Val-MEPN that is evaluated from UV–visible spectroscopy. The findings of ^{1}H NMR spectroscopy show considerable chemical shifts which confirm the strong interaction existing between the studied AAs and the drug MEPN. The detection broads up our understanding of the ordinarily discussed interfacial chemical effect of the drug MEPN and also creates a groundwork for more detailed studies of the macroscopic system behaviour, the capacity of interaction ensures its feasible area in pharmaceutical chemistry and the biomedicinal field. Moreover, a theoretical study covering the calculation of adsorption energy and establishing optimized geometry, ESP maps, and RDG specified that the hydrogen-bonding concept and hydrophobic interaction topic show favorable support in the L-Phe-MEPN composite systems which endorses the experimental findings.

Data availability statement

Data included in article/supplementary material/referenced in article.

CRediT authorship contribution statement

Baishali Saha: Writing - original draft, Investigation, Conceptualization. **Sanjoy Barman:** Investigation, Data curation. **Sukdev Majumder:** Writing - review & editing, Data curation. **Biswajit Ghosh:** Visualization. **Kangkan Mallick:** Visualization. **Subhankar Choudhury:** Writing - review & editing, Software. **Mahendra Nath Roy:** Supervision, Resources.

Declaration of competing interest

The authors declare that they have no known competing financial interests or personal relationships that could have appeared to influence the work reported in this paper.

Acknowledgments

Prof. M. N. Roy would like to acknowledge UGC, New Delhi, Government of India, for being awarded One Time Grant under Basic Scientific Research via the grant-in-Aid no. F.4-10/2010 (BSR) for providing instrumental facilities according to the research. Baishali Saha is very much grateful to Swami Vivekananda Merit Cum Means Scholarship (SVMCM), reference number WBP211628595537 for financial support to continue this research work.

Appendix A. Supplementary data

Supplementary data to this article can be found online at https://doi.org/10.1016/j.heliyon.2023.e23562.

References

[1] S. Chauhan, L. Pathania, M. Chauhan, Thermo-acoustical and optical studies of glycine and dl-alanine in aqueous furosemide solutions at different temperatures, J. Mol. Liq. 221 (2016) 755–762, https://doi.org/10.1016/j.molliq.2015.09.042.

[2] A.K. Nain, Interactions of some α-amino acids with antibacterial drug gentamicin sulphate in aqueous medium probed by using physicochemical approaches, J. Mol. Liq. 321 (2021), 114757, https://doi.org/10.1016/j.molliq.2020.114757.

[3] H. Kumar, M. Singla, R. Jindal, Studies of interionic interactions of L-serine/L- threonine in aqueous trilithium citrate solutions using density and speeds of sound measurements at different temperatures, J. Mol. Liq. 208 (2015) 170–182, https://doi.org/10.1016/j.molliq.2015.04.040.

[4] A. Sarkar, B. Sinha, Volumetric, acoustic and transport properties of metformin hydrochloride drug in aqueous D-glucose solutions at T = (298.15-318.15) K, J. Solut. Chem. 46 (2017) 424–445.

[5] J. Gupta, A.K. Nain, Physicochemical study of solute-solute and solute-solvent interactions of homologous series of α-amino acids in aqueous-isoniazid solutions at temperatures from 293.15 to 318.15 K, J. Mol. Liq. 278 (2019) 262–278, https://doi.org/10.1016/j.molliq.2019.01.036.

[6] M. Iqbal, Thermodynamic study of three pharmacologically significant drugs: density, viscosity, and refractive index measurements at different temperatures, J. Chem. Thermodyn. 41 (2) (2009) 221–226, https://doi.org/10.1016/j.jct.2008.09.016.

[7] B. Min, Q. Gao, Z. Yan, X. Han, K. Hosmer, A. Campbell, H. Zhu, Powering the remediation of the nitrogen cycle: progress and perspectives of electrochemical nitrate reduction, Ind. Eng. Chem. Res. 60 (41) (2021) 14635–14650, https://doi.org/10.1021/acs.iecr.1c03072.
[8] A.B. Khan, A. Bhattarai, Z.H. Jaffari, B. Saha, D. Kumar, Role of dimeric gemini surfactant system on kinetic study of alanine amino acid with ninhydrin reaction, Colloid Polym. Sci. 299 (2021) 1285–1294. https://link.springer.com/article/10.1007/s00396-021-04847-0.
[9] A. Basu, S. Ghosh, R. Saha, A. Ghosh, K. Mukherjee, B. Saha, Micellar catalysis of chromic acid oxidation of methionine to industrially important methylthiol in aqueous media at room temperature, Tenside Surfactants Deterg 50 (2) (2013) 94–98, https://doi.org/10.3139/113.110237.
[10] A. Bhattarai, M.A. Rub, M. Posa, B. Saha, D. Kumar, Catalytic impacts of cationic twin headed and tailed gemini surfactants toward study of glycine and ninhydrin in sodium acetate-acetic acid buffer system, J. Mol. Liq. 360 (2022), 119442, https://doi.org/10.1016/j.molliq.2022.119442.
[11] M.A. Rub, A. Bhattarai, B. Saha, Z.H. Jaffari, H.T. Thu, D. Kumar, Y.G. Alghamdi, A.M. Asiri, Effect of dicationic gemini surfactants on the rate of reaction between ninhydrin and arginine, Chem. Pap. 76 (5) (2022) 2865–2874, https://doi.org/10.1007/s11696-022-02076-5.
[12] S. Shen, H. Shi, H. Sun, Kinetics and mechanism of oxidation of the drug mephenesin by bis(hydrogenperiodato)argentate(III) complex anion, Int. J. Chem. Kinet. 39 (2007) 440–446, https://doi.org/10.1002/kin.20260.
[13] H.E. Godman, Calif. Med. 74 (1951) 126.
[14] M.C. Roy, M.N. Roy, Study to explore diverse interactions of amino acids and vitamin molecule in aqueous environment, Phys. Chem. Liq. 55 (2017) 334–346, https://doi.org/10.1080/00319104.2016.1218007.
[15] S.D. Yelamanchi, S. Jayaram, J.K. Thomas, S. Gundimeda, A.A. Khan, A. Singhal, T.S.K. Prasad, A. Pandey, B.L. Somani, H. Gowda, A pathway map of glutamate metabolism, J. Cell. Commun. Signal. 10 (1) (2016) 69–75, https://doi.org/10.1007/s12079-015-0315-5.
[16] G.R. Hedwig, The partial molar volumes and partial molar isentropic pressure coefficients of the amino acid L-asparagine in aqueous solution at the temperature 298.15 K, J. Chem. Thermodyn. 23 (2) (1991) 123–127, https://doi.org/10.1016/S0021-9614(05)80287-3.
[17] J.E. Lind Jr., J.J. Zwolenik, R.M. Fuoss, Calibration of conductance cells at 25° with aqueous solutions of potassium Chloride1, J. Am. Chem. Soc. 81 (1959) 1557–1559, https://doi.org/10.1021/ja01516a010.
[18] M. Frisch, G. Trucks, H. Schlegel, G. Scuseria, M. Robb, J. Cheeseman, G. Scalmani, V. Barone, G. Petersson, H. Nakatsuji, X. Li, Gaussian 16, Revision A. 03, Gaussian. Inc.,Wallingford CT 3 (2016).
[19] M. Deb, S. Roy, N. Hassan, J.S. Deb Roy, N.N. Ghosh, P.K. Chattopadhyay, D.K. Maiti, N.R. Singha, Chromo-fluorogenic sensing of Fe (III), Cu (II), and Hg (II) using a redox-mediated macromolecular RatiometricSensor.", ACS Appl. Polym. Mater. 7 (2023) 4820–4837, https://doi.org/10.1021/acsapm.3c00421.
[20] N.N. Ghosh, Md Habib, A. Pramanik, P. Sarkar, S. Pal, Molecular engineering of anchoring groups for designing efficient triazatruxene-based organic dye-sensitized solar cells, New J. Chem. 43 (2019) 6480–6491, https://doi.org/10.1039/C8NJ05409F.
[21] M. Cossi, V. Barone, R. Cammi, J. Tomasi, Ab initio study of solvated molecules: a new implementation of the polarizable continuum model, Chem. Phys. Lett. 255 (1996) 327–335, https://doi.org/10.1016/0009-2614(96)00349-1.
[22] J.S.D. Roy, M. Deb, M.D.H. Sanfui, S. Roy, A. Dutta, P.K. Chattopadhyay, N.N. Ghosh, S. Roy, N.R. Singha, Light-emitting redox polymers for sensing and removal- reduction of Cu (II): roles of hydrogen bonding in nonconventional fluorescence, ACS Appl. Polym. Mater. 3 (2022) 1643–1656, https://doi.org/10.1021/acsapm.1c01479.
[23] C.M. Romero, M.S. Paéz, Surface tension of aqueous solutions of alcohol and polyols at 298.15 K, Phys. Chem. Liq. 44 (2006) 61–65, https://doi.org/10.1080/01421590500315360.
[24] S. Mitra, S. Ray, N.N. Ghosh, P. Hota, A. Mukherjee, A. Bagui, D.K. Maiti, Designed and synthesized de novo ANTPABA-PDI nanomaterial as an acceptor in inverted solar cell at ambient atmosphere, Nanotechnology 34 (2023), 315704, https://doi.org/10.1088/1361-6528/acd1f8.
[25] J. Contreras-García, E.R. Johnson, S. Keinan, R. Chaudret, J.P. Piquemal, D.N. Beratan, W. Yang, NCIPLOT: a rogram for plotting noncovalent interaction regions, J. Chem. Theor. Comput. 7 (2011) 625–632, https://doi.org/10.1021/ct100641a.
[26] N. Baildya, S. Mazumdar, N.K. Mridha, A.P. Chattopadhyay, A.A. Khan, T. Dutta, M. Mandal, S.K. Chowdhury, R. Reza, N.N. Ghosh, Comparative study of the efficiency of silicon carbide, boron nitride and carbon nanotube to deliver cancerous drug, azacitidine: a DFT study, Comput. Biol. Med. 154 (2023), 106593, https://doi.org/10.1016/j.compbiomed.2023.106593.
[27] D. Ekka, M.N. Roy, Molecular interactions of α-amino acids insight into aqueous β- cyclodextrin systems, Amino Acids 45 (2013) 755–777, https://doi.org/10.1007/s00726-013-1519-8.
[28] D.O. Masson, Solute molecular volumes in relation to solvation and ionization, Philos. Mag. J. Sci. 8 (1929) 218–235, https://doi.org/10.1080/14786440808564880.
[29] A. Pal, B. Kumar, Volumetric and acoustic properties of binary mixtures of the ionic liquid 1-butyl-3-methylimidazolium tetrafluoroborate [bmim][BF4] with alkoxyalkanols at different temperatures, J. Chem. Eng. Data 57 (2012) 688–695, https://doi.org/10.1021/je2010209.
[30] L.G. Hepler, Thermal expansion and structure in water and aqueous solutions, Can. J. Chem. 47 (1969) 4613–4617, https://doi.org/10.1139/v69-762.
[31] M.N. Roy, V.K. Dakua, B. Sinha, Partial molar volumes, viscosity B-coefficients, and adiabatic compressibilities of sodium molybdate in aqueous 1, 3-dioxolane mixtures from 303.15 to 323.15 K, Int. J. Thermophys. 28 (2007) 1275–1284, https://doi.org/10.1007/s10765-007-0220-0.
[32] T. Banerjee, N. Kishore, Interactions of some amino acids with aqueous tetraethylammonium bromide at 298.15 K: a volumetric approach, J. Solution Chem. 34 (2) (2005) 137–153, https://doi.org/10.1007/s10953-005-2746-8.
[33] G. Jones, M. Dole, The viscosity of aqueous solutions of strong electrolytes with special reference to barium chloride, J. Am. Chem. Soc. 51 (1929) 2950–2964, https://doi.org/10.1021/ja01385a012.
[34] Q. Liu, L. Ma, K. Li, J. Wang, Y. Zang, Apparent molar volumes of hydrophobic imidazolium type ionic liquids with dimethyl carbonate, J. Mol. Liq. 309 (2020), 113010, https://doi.org/10.1016/j.molliq.2020.113010.
[35] F.J. Millero, Mol.kg-1 volumes of electrolytes, Chem. Rev. 71 (1971) 147–176, https://doi.org/10.1021/cr60270a001.
[36] Y. Marcus, ViscosityB-coefficients, structural entropies and heat capacities, and the effects of ions on the structure of water, J. Solut. Chem. 23 (1994) 831–848, https://doi.org/10.1007/BF00972677.
[37] H.J.V. Tyrrell, M. Kennerley, Viscosity B-coefficients between 5° and 20° for glycolamide, glycine, and N-methylated glycines in aqueous solution, J. Chem. Soc. A (1968) 2724–2728, https://doi.org/10.1039/J19680002724.
[38] R.H. Stokes, R. Mills, Viscosity of Electrolytes and Related Properties, Pergamon Press, 1965.
[39] J.M. Tsangaris, R.B. Martin, Viscosities of aqueous solutions of dipolar ions, Arch. Biochem. Biophys. 112 (1965) 267–272, https://doi.org/10.1016/0003-9861(65)90045-7.
[40] S. Glasstone, K.J. Laidler, H. Eyring, The Theory of Rate Processes, McGraw-hill, 1941.
[41] H.D.B. Jenkins, Y. Marcus, Viscosity B-coefficients of ions in solution, Chem. Rev. 95 (1995) 2695–2724, https://doi.org/10.1021/cr00040a004.
[42] U. Dash, B. Samantaray, S. Mishra, Volumetric and viscometric studies of sodium nitroprusside in aqueous solutions at different temperatures, J. Teach. Res. Chem. 11 (2005) 87–90.
[43] V.I. Minkin, Dipole Moments in Organic Chemistry, Springer Science & Business Media, 2012.
[44] M. Born, E. Wolf, Principles of Optics: Electromagnetic Theory of Propagation, Interference and Diffraction of Light, Elsevier, 2013.
[45] D. Feakins, F.M. Bates, W.E. Waghorne, K.G. Lawrence, Relative viscosities and quasi-thermodynamics of solutions of tert-butyl alcohol in the methanol–water system: a different view of the alkyl–water interaction, J. Chem. Soc. Faraday Trans. 89 (1993) 3381–3388, https://doi.org/10.1039/FT9938903381.
[46] D. Feakins, D.J. Freemantle, K.G. Lawrence, Transition state treatment of the relative viscosity of electrolytic solutions. Applications to aqueous, non-aqueous and methanol + water systems, J. Chem. Soc. Faraday Trans. 1 70 (1974) 795–806, https://doi.org/10.1039/F19747000795.
[47] A. Ali, S. Hyder, S. Sabir, D. Chand, A.K. Nain, Volumetric, viscometric, and refractive index behaviour of α-amino acids and their groups' contribution in aqueous d-glucose solution at different temperatures, J. Chem. Thermodyn. 38 (2006) 136–143, https://doi.org/10.1016/j.jct.2005.04.011.
[48] H.L. Friedman, C. Krishnan, Studies of hydrophobic bonding in aqueous alcohols: enthalpy measurements and model calculations, J. Solut. Chem. 2 (1973) 119–140.

[49] T.S. Sarma, J.C. Ahluwalia, Experimental studies on the structures of aqueous solutions of hydrophobic solutes, Chem. Soc. Rev. 2 (1973) 203–232, https://doi.org/10.1039/CS9730200203.
[50] M. Deetlefs, K.R. Seddon, M. Shara, Predicting physical properties of ionic liquids, Phys. Chem. Chem. Phys. 8 (2006) 642–649, https://doi.org/10.1039/B513453F.
[51] D. Ekka, M.N. Roy, Conductance, a contrivance to explore ion association and solvation behavior of an ionic liquid (tetrabutylphosphonium tetrafluoroborate) in acetonitrile, tetrahydrofuran, 1,3-dioxolane, and their binaries, J. Phys. Chem. B 116 (2012) 11687–11694, https://doi.org/10.1021/jp302465s.
[52] M. Mondal, S. Basak, B. Rajbanshi, S. Choudhury, N.N. Ghosh, M.N. Roy, Subsistence of diverse interactions of some biologically important molecules in aqueous ionic liquid solutions at various temperatures by experimental and theoretical investigation, J. Mol. Structure 1257 (2022), 132571, https://doi.org/10.1016/j.molstruc.2022.132571.
[53] X.M. Shen, F. Zhang, G. Dryhurst, Oxidation of dopamine in the presence of cysteine: characterization of new toxic products, Chem. Res. Toxicol. 10 (1997) 147–155, https://doi.org/10.1021/tx960145c.
[54] C.M. Romero, E. Jiménez, F. Suárez, Effect of temperature on the behavior of surface properties of alcohols in aqueous solution, J. Chem. Thermodyn. 41 (2009) 513–516, https://doi.org/10.1016/j.jct.2008.11.004.
[55] M. Mondal, S. Basak, S. Choudhury, N.N. Ghosh, M.N. Roy, Investigation of molecular interactions insight into some biologically active amino acids and aqueous solutions of an anti-malarial drug by physicochemical and theoretical approach, J. Mol. Liq. 341 (2021), 116933, https://doi.org/10.1016/j.molliq.2021.116933.
[56] R.I. Slavchov, J.K. Novev, Surface tension of concentrated electrolyte solutions, J. Colloid Interface Sci. 387 (2012) 234–243, https://doi.org/10.1016/j.jcis.2012.07.020.
[57] S. Kumar, S. Sagar, M. Gupta, A thermodynamic and 1H NMR spectroscopy study of binary mixtures of polyethylene glycol butyl ether (PEGBE) 206 with 1-Butanol and 2- (Methylamino) ethanol(MAE), J. Mol. Liq. 214 (2016) 306–312, https://doi.org/10.1016/j.molliq.2015.12.012.
[58] J. Contreras-García, E.R. Johnson, S. Keinan, R. Chaudret, J.P. Piquemal, D.N. Beratan, W. Yang, NCIPLOT: a program for plotting noncovalent interaction regions, J. Chem. Theor. Comput. 7 (3) (2011) 625–632.